

## THE CHROMOSPHERIC TEMPERATURE RISE IN FLUXTUBES

J.H.M.J. BRULS      Sterrekundig Instituut Utrecht, P.O. Box 80000,  
3508 TA Utrecht, The Netherlands

S.K. SOLANKI      Institute of Astronomy, ETH-Zentrum, CH-8092  
Zürich, Switzerland

**ABSTRACT**      We try to derive the location of the chromospheric temperature rise in fluxtubes, based on non-LTE Stokes  $V$  profile fits of medium-strong iron lines. Our preliminary conclusion is that the fluxtube chromosphere starts at about the same optical depth in the tube as in the quiet sun.

Keywords: fluxtubes; chromospheres; non-LTE line formation

INTRODUCTION

Several attempts have recently been made to infer semi-empirical models of the temperature and magnetic flux (or field strength and filling factor) in the magnetic part of the solar photosphere and lower chromosphere, either by fitting the Stokes  $V$  component of a number of line profiles assuming local thermodynamic equilibrium (LTE) to observed line profiles of network and plage regions (Stenflo 1975, Solanki 1986, Keller *et al.* 1990), or by computing non-LTE line profiles without using polarization information (Solanki *et al.* 1991).

LTE methods cannot reveal the presence of a chromospheric temperature rise because they determine the excitation temperature rather than the electron temperature. No empirical models based on non-LTE computations of Stokes  $V$  profiles exist so far. We undertake such an analysis using Fe I and Fe II Stokes  $V$  profile observations.

MODELS AND METHOD

The concept of fluxtubes makes this analysis tractable, in the sense that it allows us to use separate components for the magnetic and non-magnetic parts of the solar atmosphere in 1.5-D approximation with a limited number of vertical lines of sight sampling the composite 2-D atmosphere at different distances from the fluxtube center (*cf.* Steiner & Pizzo 1989). The external non-magnetic atmosphere around the fluxtube is represented by the Maltby *et al.* (1986) quiet sun atmosphere. We use several fluxtube models (Fig. 1), all derived from the chromosphereless NETWORK model of Solanki (1986). We employ 24 magnetically sensitive Fe I and Fe II lines that are nearly free of blends and have sufficient spread in excitation energy and equivalent width to sample different formation heights and different temperature sensitivities. For these lines we compute non-LTE Stokes profiles resulting from the 6 different fluxtube models, with 10 vertical lines of sight through each model. The radiative

transfer calculations were done in a two-step procedure, employing the field-free approximation. First a non-magnetic non-LTE source function was computed with the latest version of the Carlsson (1986) code MULTI, employing a 100-level iron model atom. That source function was then integrated using the Diagonal Element Lambda Operator (DELO) method of Rees *et al.* (1989), assuming a magnetically split line profile. Finally, the computed line profiles for all lines of sight were averaged with appropriate weights to represent a cylindrical fluxtube geometry embedded in a non-magnetic environment.

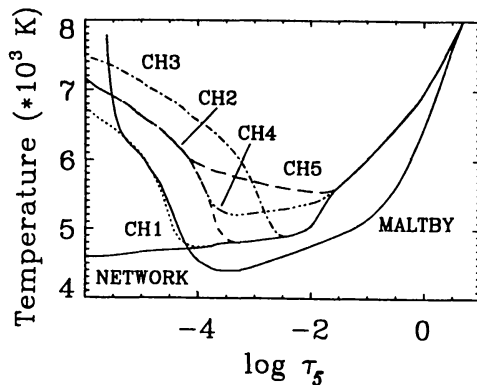


Fig. 1: Temperature stratification of fluxtube models against the optical depth at 5000 Å for each model. The chromosphereless model (solid) is the NETWORK model from Solanki (1986). The other solid curve represents the Maltby *et al.* (1986) quiet sun model. The other fluxtube models were derived by adding the chromosphere of the quiet sun model to the NETWORK model, at different heights.

## DISCUSSION

Figure 2 displays observed (solid) and computed (dashed) Stokes  $V$  components for 2 stronger lines; the computed profiles are smeared with Gaussian macroturbulence. The best, but not perfect, fit to the observed  $V$  peak widths for all of these lines is reached for  $v = 2$  km/s. All profiles are scaled such that the computed Stokes  $V$  amplitudes best fit the asymmetric observed peaks. This scaling factor is a free parameter corresponding to the magnetic filling factor, since the computed Stokes  $V$  amplitudes are directly proportional to this filling factor. Only a few computed profiles and none of the observed profiles display line-center inversions in the Stokes  $V$  component. However, these disappear with 2 km/s macroturbulent smearing, except for the Fe II 4923 line; this line requires 3 km/s to remove the inversion, which still seems a reasonable velocity. None of the models can be excluded on the basis of line center inversions.

Additionally, we look at Stokes  $V$  area ratios (Table I) for a number of well-chosen pairs of lines which differ in strength, excitation energy or ionization stage. This procedure removes the necessity to scale the computed Stokes  $V$  profiles, but still requires applying macroturbulence; we use 2 km/s for all lines. Excluding the line ratios involving lines 5405 and 5083 (for which we have problems fitting line profiles in the quiet sun), it is clear that model CH5 best fits the observed ratios, followed by CH4 and CH3. Increasing the ratios involving 5405 and 5083 by the percentage needed to bring their Stokes  $V$  amplitude scaling factors in agreement with the ones found for the other strong lines, all these 3 models do approximately equally well.

The current set of lines therefore cannot completely constrain the fluxtube temperature in the upper photosphere ( $-3 < \log \tau_5 < -2$ ). Fe II 4923 needs a low temperature near  $\log \tau_5 = -4$ , but since CH1 and CH2 do not correctly fit the other lines, our best preliminary guess is a model like CH4 (steep chromospheric

temperature rise) or CH5 (more gradual rise), but with decreasing or nearly constant  $T_e$  out to the point where it crosses CH1, and following CH1 from that point on, possibly supported by somewhat lower temperatures in the surrounding non-magnetic atmosphere as well. This agrees well with the conclusions by Solanki *et al.* (1991) based on the stronger Ca II resonance lines.

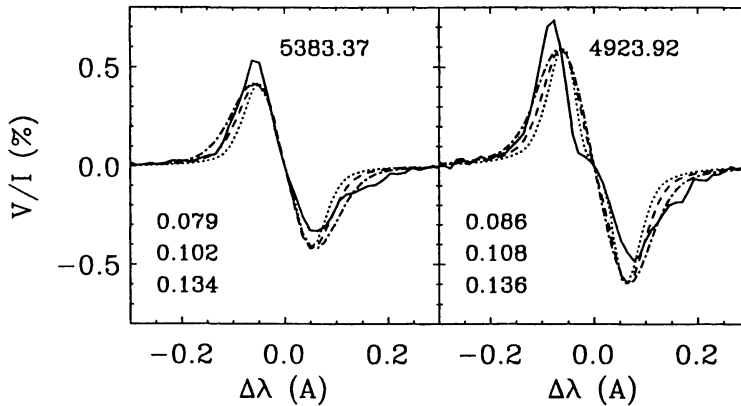


Fig. 2: Scaled Stokes  $V$  profiles. Computed profiles are smeared with 1 (dotted), 2 (dashed) and 3 km/s macro-turbulence (dot-dashed); the corresponding scale factors are shown at the lower left of each panel. We plot only NETWORK results, because the scaled profiles are virtually the same for all models.

TABLE I Stokes  $V$  area ratios

Line ratio	Observed	NETWORK	CH1	CH2	CH3	CH4	CH5
5405.772 / 5083.337	0.77	0.87	0.88	0.86	0.79	0.82	0.68
5232.938 / 5217.388	1.05	1.20	1.21	1.20	1.18	1.17	1.08
4923.925 / 5197.577	2.50	2.20	2.15	1.94	1.61	1.80	1.60
5405.772 / 5217.388	0.70	0.69	0.70	0.69	0.60	0.59	0.45
5405.772 / 5383.370	0.78	0.75	0.76	0.75	0.64	0.64	0.48
5232.938 / 5383.370	1.17	1.30	1.31	1.31	1.27	1.26	1.17
5405.772 / 5232.938	0.67	0.57	0.58	0.57	0.51	0.50	0.41
5083.337 / 5383.370	1.02	0.86	0.86	0.87	0.82	0.77	0.71
5405.772 / 5197.577	1.46	1.17	1.18	1.17	1.11	1.03	0.86
5083.337 / 5197.577	1.90	1.35	1.33	1.36	1.41	1.25	1.27
5232.938 / 5197.577	2.18	2.05	2.03	2.06	2.18	2.04	2.09
5383.370 / 5197.577	1.86	1.57	1.55	1.57	1.72	1.62	1.79

## REFERENCES

- Carlsson, M.: 1986, *Thesis. Uppsala Report No. 33*
- Keller, C. U., Solanki, S. K., Steiner, O., Stenflo, J. O.: 1990, *Astron. Astrophys.* **233**, 583
- Maltby, P., Avrett, E. H., Carlsson, M., Kjeldseth-Moe, O., Kurucz, R. L., and Loeser, R.: 1986, *Astrophys. J.*, **306**, 284
- Rees, D. E., Murphy, G. A., Durrant, C. J.: 1989, *Astrophys. J.* **339**, 1039
- Solanki, S. K.: 1986, *Astron. Astrophys.* **168**, 311
- Solanki, S. K., Steiner, O., Uitenbroek, H.: 1991, *Astron. Astrophys.*, in press
- Steiner, O., Pizzo, V.J.: 1989, *Astron. Astrophys.* **211**, 447
- Stenflo, J. O.: 1975, *Solar Phys.* **42**, 79